Production of electrons in heavy-ion–atom collisions at 40 to 120 MeV

J. A. McClintock,* Y. K. Lee, and L. Madansky
Department of Physics, The Johns Hopkins University, Baltimore, Maryland 21218
(Received 7 December 1978)

Cross sections were measured for the production of electrons with kinetic energies from 50 to 150 keV by heavy-ion–atom collisions. Beams of 40- and 70-MeV nickel and 70- and 120-MeV bromine ions were incident on targets of carbon, nickel, potassium bromide, silver, and gold. Electron energies were measured using a steering electron spectrometer capable of 7% transmission and 4-keV resolution. The observed cross sections exceed the plane-wave-Born-aproximation predictions by factors of 2 to 10 with deviation becoming more pronounced at high electron energy.

I. INTRODUCTION

Recently the K-shell ionization in heavy-ion collisions has been intensively studied.[1] The symmetric collisions, such as Br + Br, at energies slightly below Coulomb barriers, were particularly well studied in the context of molecular-orbital or promotional model.[2] Most of such studies were confined to the measurements of x-ray cross sections, and the direct observation of electron processes were rarely reported.[3] Recently, Bosch *et al.*[4] reported the evidence of energetic electrons from asymmetric collisions of S and O on Pb.

In the present paper we report a study of the electron spectra in heavy-ion collisions obtained by use of a steering-magnet electron spectrometer. A preliminary report has been published earlier.[5] The spectrometer has a high transmission and low background and is suitable for detection of rare events in heavy ion collisions. The choice of target-projectile combination of symmetric or nearly symmetric collisions was motivated to detect the signature of unified atoms.[6,7]

Several laboratories in the past reported the observation of quasimolecular x rays in heavy-ion collisions, in particular the symmetric collisions of Br + Br,[8] and the collisions Ni + Ni,[9] and interpreted the data in terms of the promotion theory of Fano and Lichten.[2] The study of K-shell ionization process in heavy-ion collisions by means of x-ray detection usually suffers from various background radiations. This situation is especially pronounced when the continuous x-ray spectrum due to united atoms is superimposed on the bremsstrahlung caused by secondary electrons and nucleus-nucleus collision, and the tail of the radiative electron capture spectra. The present study is meant to provide an independent method of studying the multitude of electron processes in heavy-ion collisions.

The main features of the k-shell ionization process in heavy-ion collisions are successfully described for our choice of beam energy by the Coulomb-ionization model.[10] In this model the incoming and outgoing projectiles are often treated as plane waves in a Born approximation (PWBA). At the first look the PWBA should have applicability when the charge of one of the colliding particles is small and the speed of the projectile is much greater than the speed of an electron in the Bohr orbit. However, the range of applicability is far greater than the above limit; this is brought about by the short interaction time due to screening.[1] A number of corrections have been added to the original formulation including the effect of Coulomb deflection of projectiles and the relativistic effects for heavy nuclei.[11] A dramatic improvement is obtained when the effect of the penetration of the projectile nucleus in the K shell of the target atom is taken into account by parametrizing the binding energy of the K-shell electrons.[12] However, comparable detailed studies of electron spectra from ion-atom collisions are not yet available.

In the present study the electron spectra above 50 keV in the symmetric collision of Br + Br and other combinations with lighter or heavier targets are presented. In most of the cases the spectrum represents a monotonic, rapidly decreasing function of electron energy, blending with the background near 100 keV. The data are compared with the scaling law predicted by PWBA without parametrizing the binding-energy increase.[13] Large deviations from such scaling laws are observed. However, no claim is made that the present data can be used to decide if the deviation is caused by quasimolecular effects, or by simple increase in binding energy due to penetration of projectile into K shell.

II. EXPERIMENTAL PROCEDURES

The energies of the electrons produced in the heavy-ion collisions were analyzed by a spectrometer using a magnetic steering field and a Si(Li)

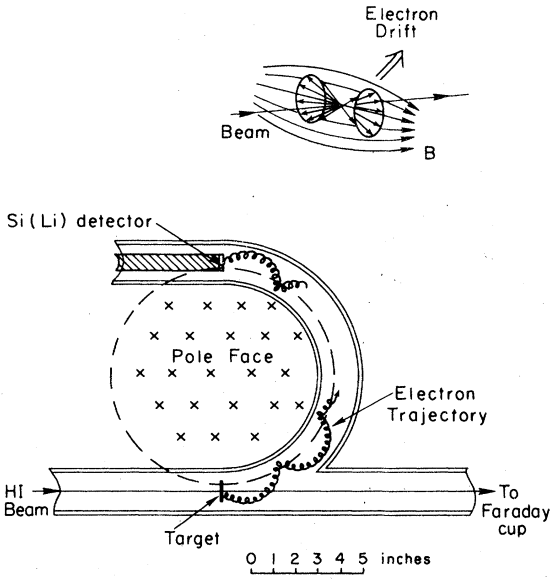

FIG. 1. Cross section of the trochoidal spectrometer. The trajectory of an electron which is emitted almost perpendicular to the magnetic field is schematically shown. The inset shows the "escape cone" of the effective magnetic bottle.

detector. The steering field was provided by circular pole pieces of 10 in. in diameter as shown in Fig. 1. In Fig. 1 the main component of the magnetic field is perpendicular to the paper. The electrons coming from the target orbit around the field lines, shown as a trochoidal trajectory in Fig. 1, but due to the fringing of the field near the edges of the magnet pole pieces, they also experience a force causing them to drift through the spectrometer and to the detector. The present configuration, in which the electrons from the target are steered around a 180° circular arc to the detector, allows good shielding of the detector from other radiations emitted at the target. A spectrometer of similar design has been described before.[14-16]

In this device one important aspect is the effective magnetic mirror due to the fringing field near the edges of the pole pieces which reflects the electrons from pole piece to pole piece, and keeps the electron cloud in a trochoidal motion as in Fig. 1. It is easy to see that electrons emitted in a direction perpendicular to the magnetic field spirals in a tight circular orbit and are more easily contained than those electrons emitted almost parallel to the magnetic field. This situation is illustrated in the inset of Fig. 1, where the "escape cone," a term used in the plasma physics of magnetic mirror machines, is shown with the axis perpendicular to the direction of the heavy-ion beam. It is seen from Fig. 1 that the spectrometer acceptance samples all angles of electron emission with respect to the beam direction.

The energy of electrons was measured by a cooled Si(Li) detector, which caused problems due to an accumulation of condensation on the surface of the Si(Li) detector. This layer generally was thicker than the target and limited the energy resolution of the system to about 4 keV. The thickness of this layer was reduced by periodic cycling of the detector to room temperature which permitted pumping away the condensed vapors.

The Si(Li) detector in the spectrometer was calibrated by internal conversion lines of radioactive sources. These sources, ^{109}Cd and ^{207}Bi, were prepared from carrier-free source material on 20-μg/cm^2 carbon foils to emulate the environment of an electron emitted during the heavy-ion experiments. The transmission function was studied by observing the continuous spectrum of β particles from ^{14}C. The Kurie plot shows excess low-energy electrons around and below 60 keV, mainly due to the energy degradation in the dead layer of the Si(Li) detector window and the condensation of water vapor on the detector. As mentioned before the detector had to be thermally recycled at the beginning of each run to eliminate the condensation. A small correction was made for energy loss due to the time dependent buildup of condensation on the counter. The transmission function used for the final analysis is obtained by the study of the Kurie plot of ^{14}C and the effect of energy degradation in the condensation layer. The transmission is flat at 6% above 100 keV and increases to 8% at 60 keV.

The targets were thin films of carbon, nickel, potassium bromide, silver, and gold prepared by vacuum evaporation. The targets ranged in thickness from about 15–50 μg/cm^2, and were supported by a 20-μg/cm^2 carbon backing foil. This backing foil was an experimental convenience which did not greatly affect the measurements. The low Z of the carbon made it relatively unimportant to the investigation as can be seen from the theoretical model. For completeness the carbon backing was included as a target constituent in the data analysis.

The beam current was monitored by integrating the transmitted beam with suitable charge state correction and also by observing the Rutherford scattering from the target foil.

A major advantage of the spectrometer is the low background in the Si(Li) detector and the spectrometer as a whole. The Si(Li) detector is insensitive to γ and neutron background and the present system uses a small and thin detector. Good shielding is provided between the target and the detector. Furthermore, the trochoidal spec-

trometer provides a clean high-energy cutoff and eliminates positrons by the nature of the steering field. Small corrections were made by measuring the room background, target-dependent background with magnet off, and target-independent background with target removed from the frame.

III. RESULTS

The bromine beams at 70 and 120 MeV were used with targets of Ni, KBr, Ag, and Au for the measurement of electron spectra as shown in Table I. The nickel beams at 70 and 40 MeV were used with a similar set of targets, as shown in Table II, to see the effect of change in projectile species, and also to study the symmetric pair of Ni on Ni.

The electron spectrum shows a continuous energy distribution rapidly decreasing as a function of electron energy, with measurable cross section to 150 keV. In the presentation of the results of measurements of the electron spectra, an attempt has been made to cast the raw data in a form that can be readily compared to theoretical models. Theoretical investigation of electron production in ion-atom collisions in the present regime of energy are rather few, although detailed studies of the total cross section for K-shell ionization exists in several different forms. A useful choice for comparisons with experiment is the plane-wave Born approximation which gives the cross section as

$$\frac{d\sigma}{dE_e}=4\pi Z_1^2\frac{M_1}{E_1}\frac{e^4}{\hbar^2}\int\left|\int_{q_{\min}}^{q_{\max}} e^{i\vec{q}\cdot\vec{r}}\psi_{k'}(\vec{r})\times\psi_k(\vec{r})\,d^3r\right|^2\frac{dq}{q^3}, \quad (1)$$

where $\psi_k(\vec{r})$ and $\psi_{k'}(\vec{r})$ are the initial- and final-electron wave functions, M_1, E_1, and z_1 are the mass, energy, and charge of the projectile, respectively. In evaluating the definite integral, we follow Torben Huus *et al.*,[13] and assume that the contribution to the cross section to lowest order in $1/q$ is from S-electronic states in the target atoms, and use the usual value of

$$\hbar q_{\min}=(E_b+E_e)(M_1/2E_1)^{1/2},$$

where E_b is the unscreened binding energy of the electron, E_e is the electron energy in the center of mass, and $q_{\max}$ is set to infinity. This permits the cross section to be calculated for S states in all subshells of the target atom which yield

$$\frac{d\sigma}{dE_e}=\frac{2^{18}\pi}{5}Z_1^2e^4\left(\frac{M_eE_1}{M_1}\right)^4\frac{nE_b}{(E_b+E_e)^{10}}. \quad (2)$$

To use the above formula in a laboratory system one should convert E_e to laboratory energy. In view of the fact that the transmission of the trochoidal spectrometer averages over the emis-

TABLE I. Comparison of the electron-production cross section to the predictions of PWBA for Br beam experiment. The measured cross section which is divided by the PWBA prediction is shown for various projectile-target combinations at two beam energies. The values for each combination are normalized to one at the electron energy of 52 keV for convenience. The statistical uncertainties are given in parentheses and correspond to the last effective numbers of the data.

Electron energy keV	Br Beam at 120 MeV Targets					Br Beam at 70 MeV Targets			
	C	Ni	KBr	Ag	Au	Ni	KBr	Ag	Au
52	1.00(1)	1.00(1)	1.00(1)	1.00(1)	1.00(1)	1.00(3)	1.00(3)	1.00(4)	1.00(1)
56	1.16(2)	1.13(2)	1.23(1)	1.18(2)	1.20(1)	1.23(4)	1.02(4)	1.23(5)	1.28(2)
60	1.32(2)	1.25(3)	1.48(1)	1.34(2)	1.47(1)	1.44(6)	1.13(6)	1.45(7)	1.66(3)
64	1.40(3)	1.35(4)	1.74(1)	1.52(4)	1.70(2)	1.64(8)	1.20(8)	1.68(1)	2.07(5)
68	1.72(4)	1.42(5)	2.01(2)	1.75(5)	1.98(3)	1.87(12)	0.99(8)	2.03(15)	2.59(7)
72	1.82(6)	1.72(8)	2.31(3)	1.86(7)	2.24(4)	2.05(15)	1.39(13)	2.36(20)	3.00(9)
76	1.95(8)	1.61(9)	2.61(3)	2.03(9)	2.56(5)	2.32(21)	2.03(22)	2.55(26)	3.39(12)
80	2.33(10)	2.32(14)	2.92(4)	2.05(11)	2.85(7)	2.57(28)	2.05(27)	2.73(33)	3.76(16)
84	2.68(14)	3.15(20)	3.19(6)	2.25(15)	3.20(10)	3.38(40)	2.25(33)	3.31(45)	4.24(21)
88	2.79(18)	2.65(23)	3.29(7)	2.29(17)	3.60(13)	4.11(54)	2.29(39)	3.57(56)	4.13(25)
92	3.48(24)	2.19(25)	3.78(9)	2.11(20)	4.09(16)	3.82(64)	2.11(44)	3.76(70)	4.59(32)
96	3.62(29)	2.16(30)	3.85(11)	2.41(26)	4.25(20)	5.42(93)	2.41(60)	3.25(77)	4.98(40)
100	4.40(39)	2.21(37)	4.07(14)	1.97(24)	4.23(23)	5.3(11)	1.97(49)	3.08(90)	5.43(49)
104			4.24(17)		4.80(30)				5.52(59)
108			4.41(20)		4.34(31)				5.31(68)
112			4.61(26)		4.34(38)				
116					4.50(44)				
120					4.44(51)				

TABLE II. Comparison of the electron-production cross section to the predictions of PWBA for Ni beam experiment. For explanation, see the caption for Table I.

Electron energy keV	Ni Beam at 70 MeV Targets Ni	KBr	Au	Ni Beam at 40 MeV Targets Ni	KBr	Ag	Au
52	1.00(2)	1.00(2)	1.00(2)	1.00(10)	1.00(10)	1.00(6)	1.00(4)
56	1.20(4)	1.21(4)	1.18(3)	1.27(15)	1.37(15)	1.22(8)	1.36(7)
60	1.37(5)	1.41(5)	1.34(5)	1.49(22)	1.70(23)	1.45(12)	1.72(10)
64	1.53(7)	1.51(7)	1.49(7)	1.44(29)	1.76(32)	1.73(17)	2.27(16)
68	1.70(10)	1.57(10)	1.55(9)	1.36(37)	1.67(35)	2.03(24)	2.88(23)
72	1.75(13)	1.69(13)	1.33(10)	1.80(54)	2.20(48)	2.16(32)	3.02(30)
76	1.84(17)	1.76(16)	1.19(12)	2.04(73)	2.50(70)	2.34(42)	3.17(38)
80	1.83(22)	2.08(23)	1.19(17)	2.9(11)	3.54(96)	3.08(58)	3.48(49)
84	2.07(29)	2.28(30)	0.94(17)	3.8(16)	4.6(13)	4.09(82)	3.45(62)
88	1.78(33)	2.49(39)		1.4(12)	1.71(55)	3.58(93)	3.64(76)
92	2.46(47)	2.65(49)				4.2(12)	3.17(86)
96	2.73(61)	3.39(67)				5.7(17)	3.2(10)
100	3.62(84)	3.13(77)				4.8(19)	
104		4.6(11)				7.0(27)	

sion angle of the electrons the expression becomes rather involved, but the correction is of the order of the energy of the electron moving with the center of mass $\frac{1}{2}m_e V^2_{\text{c.m.}}$, which is small.[15]

The measured cross section was derived from the formula

$$\frac{d\sigma}{dE_e} = \frac{N}{Qn\epsilon\tau} . \tag{3}$$

In this formula N is the observed counts per chan-

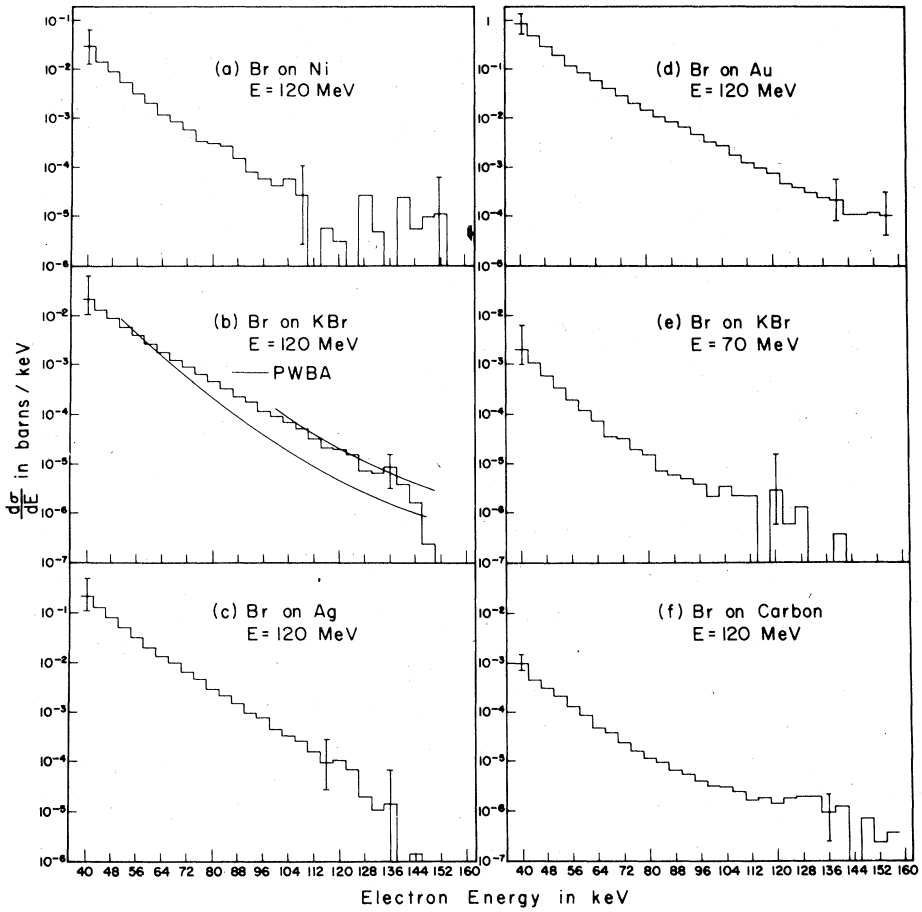

FIG. 2. Electron production cross sections for various targets with Br beam at two different beam energies. Solid lines in (b) are the best fits to PWBA for the symmetric collisions of Br on KBr at 120 MeV with one adjustable parameter; the lower line is the best fit from 50 to 150 keV, and the upper line is the best fit from 100 to 150 keV. The error bars at low-electron energy are due to systematics; the error bars at high-electron energy include counting statistics as well as systematic errors.

nel of the spectrum, Q is the number of projectiles, n is the number of target particles, ϵ is the number of keV per channel, and τ is the transmission factor which is a slowly varying function of the electron energy. The results of this computation were compared with the PWBA which was calculated by summing terms given by Eq. (2) over the K, L, M, and N shells of both the target and projectile where such sum was applicable.

In view of the rather modest progress in the theoretical model based on PWBA, we deemphasize the theoretical prediction of the absolute value for the cross sections, and focus our attention on the spectral shape. The simultaneous detection of the whole range of electron spectrum makes the present device suitable for the study of spectrum shape. The beam was monitored by both a Faraday cup and by Rutherford-scattered ions.

The electron spectra for various targets with Br beams at two different energies are shown in Fig. 2. For the case of electron spectrum of 120-MeV bromine ion incident on a potassium bromide target, the theoretical curves by PWBA are shown in Fig. 2(b). The solid lines represent the prediction of PWBA with one adjustable parameter to best fit the data. The lower solid line was the best fit of PWBA for the electron energy range from 50 to 150 keV, while the upper was the best fit for the range from 100 to 150 keV. The one adjustable parameter is the total number of events, and therefore can be interpreted as allowing the target thickness or the number of beam particles to vary.

The observed cross sections were compared with predictions of the PWBA by dividing the measured counting rate by the PWBA predictions. The results are normalized to 1 at the electron energy of 52 keV for convenience and are presented in Tables I and II. These numbers represent our best estimates for the cross sections. In Tables I and II the uncertainties represent the counting statistics only. Since the systematic errors are large they are indicated by error bars in Fig. 2. In Fig. 2 the low-energy error bars are due entirely to systematics while the high-energy error bars include the statistical error. The data were corrected for the effect of the carbon backing which was in all cases an order of magnitude smaller than the spectra of interest. The electron spectrum with the carbon backing alone as a target is also shown in Fig. 2(f) for the 120-MeV Br beam. For all projectile-target combinations there is a systematic enhancement of the cross section over the PWBA approximation as a function of electron energy. The PWBA has a greater deviation from the observations at high-electron energy than at the lower energies. In all the regions of observation the Born approximation underestimates the observed cross section. The systematic errors which could contribute to this effect include the absorption by condensed material on the detector and the energy-dependent transmission function, as discussed in Sec. II.

So far we have ignored possible angular distribution of electrons dependent on electron energy. The transmission function for the spectrometer tends to average over the emission angle with respect to the beam direction, but prefers the electrons emitted in the direction perpendicular to the magnetic field direction as described in Sec. II. As a rough estimate of the effect of angular distribution, consider the unlikely situation where all the electrons are emitted within a 30° forward cone. Such a situation will enhance the transmission by a factor of 3.8. However, it is clear that a future experiment should take into account the angular distribution of electrons.

Further theoretical considerations of electron production in ion-atom collision is necessary, possibly along the line of development of the theory of K-shell ionization.[12] The major correction suggested is the effect of increase in binding energy as the projectile penetrates the K shell, as it is known to modify the ionization cross section by orders of magnitude in some cases.[12] The most tightly bound electrons contribute to the cross section much more significantly at higher emitted electron energies, so that the increased deviation at higher energies observed in this experiment is at least in the right direction. It is further noted that the heavier targets have a greater divergence from the Born approximation.

IV. CONCLUSIONS

The steering magnet spectrometer with a solid-state detector proved itself to have a sufficient efficiency and energy resolution for the study of the soft electron spectra in heavy-ion collisions. In fact, there is room for further improvement in transmission and in signal-to-noise ratio. Unfortunately, the nature of the collection of electrons in a trochoidal spectrometer averages over the emission angles so that the angular-distribution information is lost, which sets a limitation in the interpretation of the results from this experiment. However, the present results on electron spectra of Br on Br clearly indicate that the scaling behavior of the electron spectra extending several times beyond the binding energy should be understood in terms of the effects of the combined atom. Any interpretation, therefore, should take into account the increased binding due to two nuclei inside the same K shell, along the line of theory developed for combined atom x rays.

ACKNOWLEDGMENTS

The authors are deeply indebted to Dr. Harry Gove for his interest in this project and to the Tandem Accelerator staff of the University of Rochester. The authors also wish to acknowledge the help rendered by A. J. Caffrey, F. D. Correll, and D. Musser in running the experiment. The present project is partly supported by the Department of Energy.

---

*Present address: Martin Marietta Laboratories, 1450 South Rolling Rd., Baltimore, Md. 21227.

[1]W. E. Meyerhof and K. Taulbjerg, Ann. Rev. Nucl. Sci. 27, 279 (1977).
[2]U. Fano and W. Lichten, Phys. Rev. 14, 627 (1965).
[3]N. Stolterfoht, D. Schneider, D. Burch, H. Wiejan, and J. S. Risley, Phys. Rev. Lett. 33, 59 (1974).
[4]F. Bosch, H. Krimm, B. Martin, B. Pvh, and T. Walcher, Phys. Lett. 78B, 568 (1978).
[5]J. A. McClintock, A. J. Caffrey, F. D. Correll, Y. K. Lee, L. Madansky, and D. Musser, Bull. Am. Phys. Soc. 22, 83 (1977).
[6]S. S. Gershtein, V. S. Popov, Lett. Nuovo Cimento 6, 593 (1973).
[7]H. Peitz, B. Müller, J. Rafelski, W. Greiner, Lett. Nuovo Cimento 8, 37 (1973).
[8]W. E. Meyerhof, T. K. Saylor, S. M. Lazarus, A. Little, B. B. Triplett, L. F. Chase, Jr., R. Anholt, Phys. Rev. Lett. 32, 1279 (1974).
[9]J. S. Greenberg, C. K. Davis, S. P. Vincent, Phys. Rev. Lett. 32, 1473 (1974).
[10]E. Merzbacher and H. Lewis, *Encyclopedia of Physics*, edited by S. Flügge (Springer-Verlag, Berlin, 1958), Vol. 34, p. 166.
[11]G. Basbas, W. Brandt, and R. Laubert, Phys. Rev. A 7, 983 (1973).
[12]F. E. McDaniel, J. L. Duggan, P. D. Miller, and G. D. Alton, Phys. Rev. A15, 846 (1977).
[13]Torben Huus, Jørgen H. Bjerregaard, and Bent Elbek, K. Dan. Vidensk. Selsk. Mat. Fys. Medd. 30, 55 (1956).
[14]K. G. Malfors, Ark. Fys. 13, 237 (1958).
[15]R. L. Watson, J. O. Rasmussen, H. R. Bowman, and S. G. Thompson, Rev. Sci. Instrum. 38, 905 (1967).
[16]Y. Gono, D. R. Zolnowski, D. R. Haenni, and T. T. Sugihara, in *Proceedings of the International Conference on Reactions Between Complex Nuclei, 1974*, edited by R. L. Robinson, F. K. McGowan, J. B. Ball, and J. H. Hamilton (North-Holland, Amsterdam, 1974), Vol. 1, p. 157.